Available online at www.sciencedirect.com
SCIENCE DIRECT®
Neuropharmacology 50 (2006) 209–218
NEURO PHARMACOLOGY
www.elsevier.com/locate/neuropharm

Galanin receptor-1 knockout mice exhibit spontaneous epilepsy, abnormal EEGs and altered inhibition in the hippocampus

Craig D. McColl [a], Arie S. Jacoby [b], John Shine [b], Tiina P. Iismaa [b], John M. Bekkers [a,*]

[a] *Division of Neuroscience, John Curtin School of Medical Research, The Australian National University, Building 54, Canberra ACT 0200, Australia*
[b] *The Garvan Institute of Medical Research, St. Vincent's Hospital, Sydney NSW 2010, Australia*

Received 17 December 2004; received in revised form 16 July 2005; accepted 2 September 2005

Abstract

Galanin is a widely-distributed neuropeptide that acts as an endogenous anticonvulsant. We have recently generated a galanin receptor type 1 knockout mouse (*Galr1*$^{-/-}$) that develops spontaneous seizures. Our aim here was to characterize the seizures by making electroencephalogram (EEG) recordings from this animal, and also to elucidate the cellular basis of its epileptic phenotype by studying the neurophysiology of CA1 pyramidal neurons in acute hippocampal slices. EEGs showed that major seizures had a partial onset with secondary generalization, and that paroxysms of spike-and-slow waves occurred and were associated with hypoactivity. The interictal EEG was also abnormal, with a marked excess of spike-and-slow waves. Slice experiments showed that resting potential, input resistance, intrinsic excitability, paired-pulse facilitation of excitatory and inhibitory postsynaptic currents (EPSCs and IPSCs), stimulus–response plots for EPSCs, and several properties of spontaneous miniature EPSCs and IPSCs were all unchanged in the mutant mouse compared with wildtype. However, the frequency of miniature IPSCs was significantly reduced in the mutants. These results suggest that impaired synaptic inhibition in the hippocampus may contribute to the local onset of seizures in the *Galr1*$^{-/-}$ mouse.

Keywords: CA1; Electroencephalogram; Excitability; Pyramidal cell; Seizure; Synaptic current

1. Introduction

Every neurologist is familiar with the need for better pharmacological agents for treating epilepsy. Approximately 30% of epileptic patients continue to have seizures despite medication and, in others, seizure control can only be obtained at the expense of unwelcome side effects, including sedation and cognitive impairment (Sander, 2004). This reflects the fact that many antiepileptic drugs either facilitate the inhibitory action of γ-amino-butyric acid (GABA) or inhibit voltage-activated sodium channels (Macdonald, 1999). Because such drugs are directed against universal mechanisms involved in controlling neuronal excitability, it is inevitable that they will inhibit normal, as well as epileptogenic, neuronal activity. It might be useful to develop anticonvulsant agents acting on transmitter systems that are anatomically more restricted and less vital for normal neurological function.

The need for novel antiepileptic drugs accounts for some of the growing interest in neuropeptide receptors as potential therapeutic targets. Galanin is a 29–30-amino acid neuropeptide that acts as an endogenous anticonvulsant in several models of hippocampal seizures (Mazarati, 2004), raising the hope that galanin agonists might eventually prove effective against the most common form of focal epilepsy, temporal lobe epilepsy. Galanin is expressed in the central and peripheral nervous system, as well as other tissues, and it has been implicated in a number of physiological processes including feeding, nociception, hormone secretion, nerve regeneration,

* Corresponding author. Tel.: +61 2 6125 2502; fax: +61 2 6125 8077.
E-mail address: john.bekkers@anu.edu.au (J.M. Bekkers).

0028-3908/$ - see front matter © 2005 Elsevier Ltd. All rights reserved.
doi:10.1016/j.neuropharm.2005.09.001

neuronal excitability and memory (for reviews see Crawley, 1996; Iismaa and Shine, 1998; Branchek et al., 2000; Wynick et al., 2001). Three galanin receptor subtypes, GalR1–3, have been cloned to date, all of them belonging to the superfamily of seven transmembrane-domain G protein-coupled receptors (Branchek et al., 2000). In the brain, the dominant sites of expression for galanin receptors are the hippocampus, subiculum and basal forebrain (Iismaa and Shine, 1998; Branchek et al., 2000; Wynick et al., 2001; Hohmann et al., 2003), which are sites implicated in the initiation and early spread of temporal lobe seizures. There is also strong expression in the hypothalamus (Mennicken et al., 2002), where galanin appears to play a role in the regulation of appetite. Each of the three known receptors has a distinct distribution and may eventually offer a distinct pharmacological target. In the hippocampus of rats and mice, the dominant galanin receptor subtypes are GalR1 in the ventral CA1 region and GalR2 in the dentate gyrus (Parker et al., 1995; O'Donnell et al., 1999; Hohmann et al., 2003; Jungnickel and Gundlach, 2005). The GalR3 receptor has a very limited distribution in the brain but it is found in the basal and limbic forebrain, septum and hypothalamus (Mennicken et al., 2002).

When injected into the hippocampus, galanin potently inhibits the induction and maintenance of kindled seizures (Mazarati et al., 1992, 1998; Mazarati and Wasterlain, 2002; Wasterlain et al., 2002). Transgenic mice engineered to overexpress the galanin gene also exhibit increased resistance to induced seizures (Mazarati et al., 2000; Kokaia et al., 2001) and adenoviral vectors expressing galanin protect mice from seizures (Haberman et al., 2003). Conversely, mice with a targeted disruption of the galanin gene are more likely to develop seizures after several different induction protocols (Mazarati et al., 2000).

In order to understand how galanin has these and other effects on the nervous system, it will be informative to study galanin receptors. The paucity of high-affinity subtype-specific ligands for these receptors (Branchek et al., 2000) led us to generate mice with a targeted disruption of the gene encoding GalR1 (*Galr1*) (Jacoby et al., 2002a,b). We found that a proportion of these animals developed severe spontaneous seizures with a mean onset age of about 11 weeks (Jacoby et al., 2002a), a result in accord with earlier data implicating galanin as an endogenous anticonvulsant. Unlike many other rodent models of epilepsy, GalR1 knockout mice appear to have partial seizures with secondary generalization, based on their seizure semiology and as confirmed in this study using multichannel electroencephalography. Thus, the $Galr1^{-/-}$ mouse may be a useful addition to the repertoire of animal models used in epilepsy research, particularly if the reasons for its seizures can be determined. Furthermore, an understanding of the mechanistic basis of epilepsy in these mice could clarify the potential for therapeutic manipulation of galanin receptors in the treatment of epilepsy and other disorders.

Here we describe a series of experiments designed to characterize further the $Galr1^{-/-}$ mouse, both at the whole-animal level, using EEG recordings, and at the cellular level, using patch clamping in brain slices. In the EEG experiments, we found a variety of striking abnormalities in the mutant animals, ranging from barrages of spike-and-slow wave discharges to fully-developed seizures characterized by a focal onset, secondary generalization and rhythmic synchronization, followed by eventual post-ictal flattening. In the slice experiments, we focused on pyramidal neurons in the CA1 region of ventral hippocampus, for three reasons. First, these neurons have been reported normally to contain a high density of GalR1 (Parker et al., 1995; Schött et al., 2000; Jungnickel and Gundlach, 2005). Second, exogenous galanin was especially effective in preventing seizures when applied to the hippocampus (Mazarati et al., 1992) and in ameliorating seizures induced by electrical stimulation of a major hippocampal input, the perforant pathway (Mazarati et al., 2004a). Third, up-regulation of galanin has been observed in the hippocampus following induced seizures (Mazarati et al., 1998). Our experiments show that several important indicators of excitability and synaptic strength are unaltered in the $Galr1^{-/-}$ mouse, but one measure of synaptic inhibition is significantly reduced in the mutant.

2. Materials and methods

2.1. Animals

All experiments used seizure-prone $Galr1^{-/-}$ mice from a mixed 129T2 and C57BL/6J background, and age-matched wildtype controls descended from the same original litters, as described previously (Jacoby et al., 2002a,b). Galanin binding is dramatically reduced in these $Galr1^{-/-}$ mice (Jungnickel and Gundlach, 2005), confirming functional loss of GalR1. In the original founding colony the penetrance of the epileptic phenotype was estimated to be 25%, averaged across several breeding lines. Further experience has shown that the penetrance varies from one breeding line to another, so that some colonies of our $Galr1^{-/-}$ mice have approximately 100% penetrance (as in this study), while others have no overt spontaneous seizures (Mazarati et al., 2004b). In the work described here, all mutant mice were observed to have convulsive seizures. Animal ages ranged from 6 to 11 months.

2.2. EEG experiments

The EEG experiments used seven $Galr1^{-/-}$ mice and nine age-matched wildtype controls. In procedures approved by the Animal Experimentation Ethics Committee (AEEC) of The Australian National University, the animals were deeply sedated with an i.p. injection of 2% chloral hydrate (0.02 ml/g), the skull was exposed, and six small holes were drilled in a 2×3 array to expose the dura mater. All six holes were 1.5 mm lateral to the midline and consisted of an anterior pair (1.5 mm anterior to bregma), a middle pair (0.5 mm posterior to bregma) and a posterior pair (2.5 mm posterior to bregma). A shallow seventh hole was drilled into the occiput, 1 mm posterior to lambda, for placement of a reference electrode (Fig. 1). Tungsten recording electrodes were placed on the dura and fixed in place with dental cement, leaving short prongs exposed for later attachment of EEG recording leads.

Multichannel EEG recordings were made after 3–7 days of recovery, in the absence of any pharmacological agents. At least 3 h of EEG were recorded for each mouse, over multiple sessions of 90 min each (although some mice with frequent seizures were subsequently observed for extra sessions). Many mice had infrequent convulsive seizures (less than once per week) so the primary aim of this work was to identify differences in the interictal EEGs of mutant and wildtype mice. Recording leads were supported above the mouse, allowing normal exploratory and grooming behavior within the recording cage. The voltage difference between each active electrode and the occipital reference electrode was amplified and recorded with a Digidata 1321A digitizer and Clampex software (Axon Instruments, Union City, CA), at a sampling

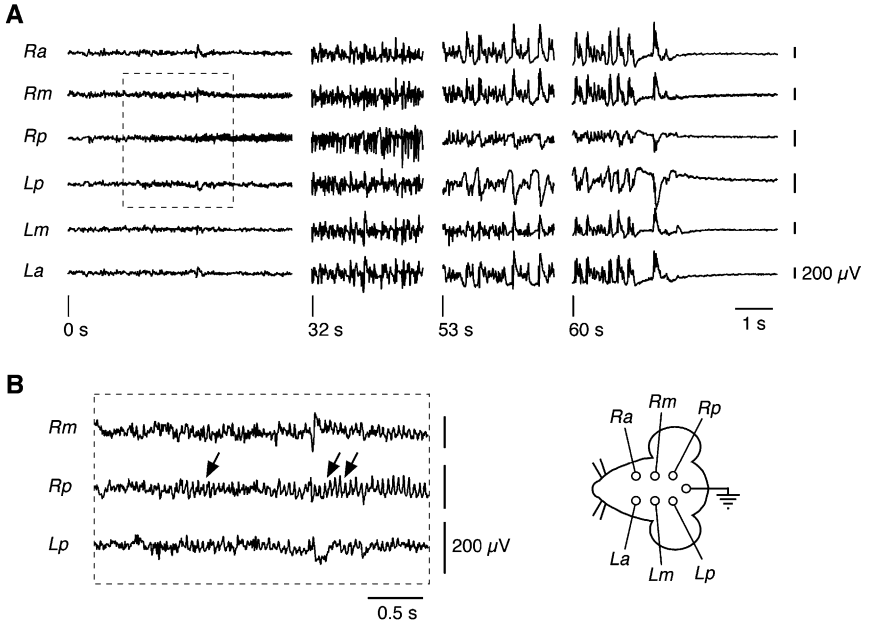

Fig. 1. EEGs recorded during a major spontaneous seizure in a *Galr1*$^{-/-}$ mouse have a localized onset and rapidly generalize. (A) EEGs recorded simultaneously from six electrodes located as shown in the pictogram at lower right. Note the progression of the seizure from onset (near 0 s), through spread (32 s) and synchronization (53 s), to termination and post-ictal flattening (60 s). (B) Expanded view of the boxed region from panel A, showing the onset of the seizure. Rhythmic electrical activity first appears in the right posterior (Rp) electrode (arrows). Inspection of the video recording shows that the animal abruptly stops moving at this time.

rate of 2 kHz. To quantify movement of the mouse, a piezoelectric tension strap (Kent Scientific, Torrington, CT) was attached to the headpiece and the output was recorded as a seventh data channel. This device was highly sensitive and was able to detect small nods of the mouse's head that were barely visible to the naked eye. Each mouse was video taped to allow visual inspection of seizure behavior and to exclude possible instances of movement artefact affecting the EEG trace.

All EEG recordings were inspected visually at a resolution of 10 s per sweep and the traces were also subjected to semi-automated analysis with Matlab software (The Mathworks Inc., Natick, MA). Spike-and-slow wave (SSW) complexes were detected using a template-matching algorithm (Clements and Bekkers, 1997), in three stages: first, a template was selected for each channel from each mouse using a simple amplitude threshold, followed by manual rejection of misshapen events and averaging of the remaining events; second, the resulting template was used to search automatically the entire EEG record for each channel for each mouse, and events closely matching the template were averaged to produce a final template for each channel and for each mouse; third, templates for all mice were averaged for each EEG channel, to produce a spike-and-slow wave template specific for each electrode position, and these templates were used for final automated detection of SSW events. A separate analysis was also performed in which each mouse was used to generate its own templates without averaging templates across all mice; this analysis produced very similar results to those reported here. The threshold criterion for the template-matching algorithm was set at 4.5 times the standard deviation of the noise as this threshold most closely matched the decisions made by visual inspection (Clements and Bekkers, 1997). Events that were misshapen or which appeared to be due to movement artefact were rejected by inspection of each event. High frequency spikes occurring within major convulsive seizures were automatically excluded from this analysis as they were too close together temporally and did not match the template, which was derived from averaged interictal EEG. All analyses were done by an experienced EEG reader blinded to the genotype of each animal.

The movement trace produced by the piezoelectric strain gauge had an irregular sinusoidal appearance, with sudden or large movements characterized by extreme departures from the baseline, usually followed by a steep return and overshoot (Fig. 2A, B). At different times, either extreme values in the raw movement trace or extreme gradients in the trace correlated best with the instantaneous movement of the mouse. Thus, to quantify movement in each recording session, both the absolute value of the raw trace and the absolute value of the first derivative of the trace were independently normalized to zero mean and unitary standard deviation; a normalized movement trace was then produced by taking the instantaneous maximum of these two results. For illustrative purposes (Fig. 2C), the resulting movement score was renormalized so that a score of 0 was assigned to the minimum movement recorded in each session and a score of 1 was assigned to the maximum movement. Statistical comparisons used the two-tailed *t*-test, with significance at $p = 0.05$. Errors are given as $\pm$SE, with n being the number of mice.

2.3. Slice experiments

Some slice experiments used animals from which EEGs had previously been recorded. Slices were prepared using standard techniques that were approved by the AEEC of The Australian National University (Bekkers and Delaney, 2001). Briefly, animals were anesthetized with 2% Fluothane in O_2, decapitated, and the brain rapidly removed into high-Mg/low-Ca ice-cold artificial cerebrospinal fluid (ACSF) containing (in mM) 125 NaCl, 3 KCl, 25 $NaHCO_3$, 1.25 NaH_2PO_4, 6 $MgCl_2$, 0.5 $CaCl_2$, 25 glucose, pH 7.4 when saturated with 95% O_2/5% CO_2. Horizontal slices (300 μm thick) were cut from the ventral hippocampus, incubated at 35 °C for 1 h in high-Mg/low-Ca ACSF, then maintained at 23–25 °C before use.

For recording, slices were continuously superfused with normal ACSF (as above except with 1 mM $MgCl_2$, 2 mM $CaCl_2$), bubbled with 95% O_2/5% CO_2 and maintained at 32–34 °C. For measuring action potentials and EPSCs, patch electrodes (3–4 MΩ) contained (in mM) 135 potassium methylsulfate, 7 NaCl, 0.1 EGTA, 2 MgATP, 0.3 GTP, 10 HEPES adjusted to pH 7.2 with KOH. For measuring IPSCs, the electrode solution contained 135 mM KCl instead of potassium methylsulfate, and 5 μM 6-cyano-7-nitroquinoxaline-2,3-dione (CNQX) was added to the ACSF. Hippocampal CA1 pyramidal neurons were identified and patch electrodes positioned using infrared/differential interference contrast (IR-DIC) videomicroscopy. Recordings were made with a MultiClamp 700A computer-controlled patch clamp amplifier (Axon Instruments). Current clamp recordings in whole-cell mode used bridge balance and capacitance neutralization, which were checked throughout the experiment.

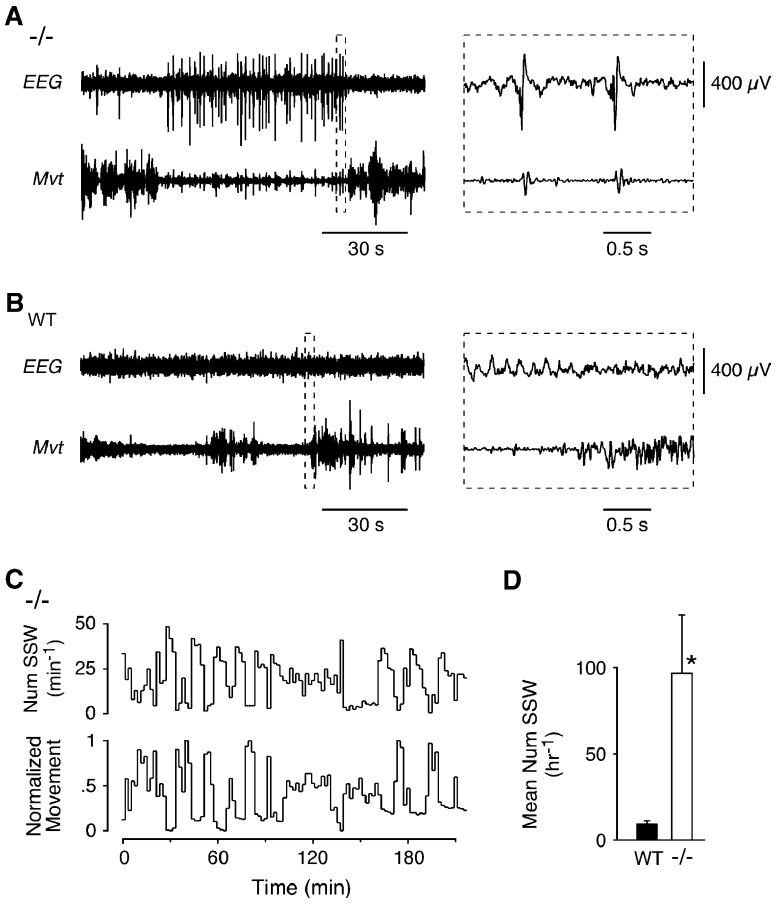

Fig. 2. Spike-and-slow wave (SSW) events are more frequent in −/− mice and are correlated with hypoactivity. (A) EEG (from Lm electrode) and associated movement trace recorded in a −/− mouse. During a ∼60-s-long flurry of SSW events the animal is motionless, apart from a clonic jerk that often accompanies each SSW. Normal movement precedes and follows this 60 s period. The segment in the dashed box (left) is shown horizontally expanded at right. This shows the structure of SSW events (top trace) and the associated clonic jerks (bottom trace). (B) Similar recordings made from a normal control mouse. SSW events are not apparent, and periods of hypoactivity are not correlated with abnormalities in the EEG. (C) Timecourse plot for the −/− animal in panel A. This shows (top) the number of SSW events on the Lm electrode per minute, and (bottom) a normalized measure of animal movement, both averaged over 2-min time bins. There is a strong inverse correlation between SSW number and animal movement over the entire period of monitoring ($r = -0.77$ by Pearson's correlation coefficient). (D) Mean number of SSW events counted per hour in the most active channel for WT (9 ± 2, $n = 9$) and −/− mice (97 ± 33, $n = 7$). The number of SSW events is significantly greater in the −/− animals ($p = 0.02$).

For measuring the properties of action potentials (APs), current steps (1 s long) were applied at 10 s intervals in 20 pA increments. The slow afterhyperpolarization was measured as the peak hyperpolarization following a 200-ms-long 500 pA current step applied at the resting potential. Recordings were filtered at 10 kHz and digitized at 20–50 kHz. Voltage clamp recordings were made at a holding potential of −60 or −70 mV. Series resistance compensation was not required for these small (<150 pA) synaptic currents. EPSCs or IPSCs were evoked at 4 or 5 s intervals by a stimulator placed in *Stratum radiatum*, filtered at 5 kHz and digitized at 10 kHz. The stimulator was a patch electrode coated with electrically conductive paint and filled with 1 M NaCl. The stimulus was a 100-μs-long current step (0–30 μA) provided by a constant-current unit. For paired-pulse experiments (Fig. 4A), the complete stimulus pattern was repeated five times and the resultant currents were averaged together. For the EPSC stimulus–response experiment (Fig. 4B), stimulus settings were interleaved in a pseudo-random sequence, with 20 or 30 EPSCs recorded during two or three visits to each setting and averaged. Membrane potentials have not been corrected for the junction potential, measured at −7 mV for these solutions.

Analysis was done using AxoGraph 4.9 (Axon Instruments) and Igor Pro 4.0 (Wavemetrics, Lake Oswego, OR). Input resistance was estimated by measuring the membrane potential at the end of a series of 1 s long, small (<40 pA) hyperpolarizing current steps, then fitting a straight line to the resultant voltage–current plot. Instantaneous AP frequency during each current step was found by averaging the reciprocal of time intervals between successive APs during that step. AP voltage threshold, AP height and afterhyperpolarization (AHP) amplitude (Fig. 3) were averaged from the APs in the first current step (increased in 20 pA increments) that generated at least three APs. The voltage threshold of an AP was defined as the linearly interpolated membrane potential, V_m, at which $dV_m/dt = 50$ V s^{-1}; this criterion gave the best agreement with threshold determinations done by eye. AP risetime was defined as the time between the voltage threshold and peak of the AP, while AP height was the amplitude difference between the same two points. The AHP amplitude was measured at the minimum voltage between adjacent APs. Amplitudes of evoked synaptic currents were measured by averaging over a 0.5–1-ms-long window around the peak. The amplitude of the second synaptic current in paired-pulse experiments (Fig. 4A) was measured after subtracting an averaged timecourse of the first synaptic current to correct for temporal overlap. Spontaneous miniature synaptic currents were detected in 90–100 s-long current records by digitally filtering at 3 kHz, then applying the template detection algorithm implemented in AxoGraph, with the threshold criterion set at four times the standard deviation of the noise (Clements and Bekkers, 1997). Statistical comparisons used the two-tailed *t*-test, with significance at $p = 0.05$. Errors are given as ±SE, with n being the number of cells.

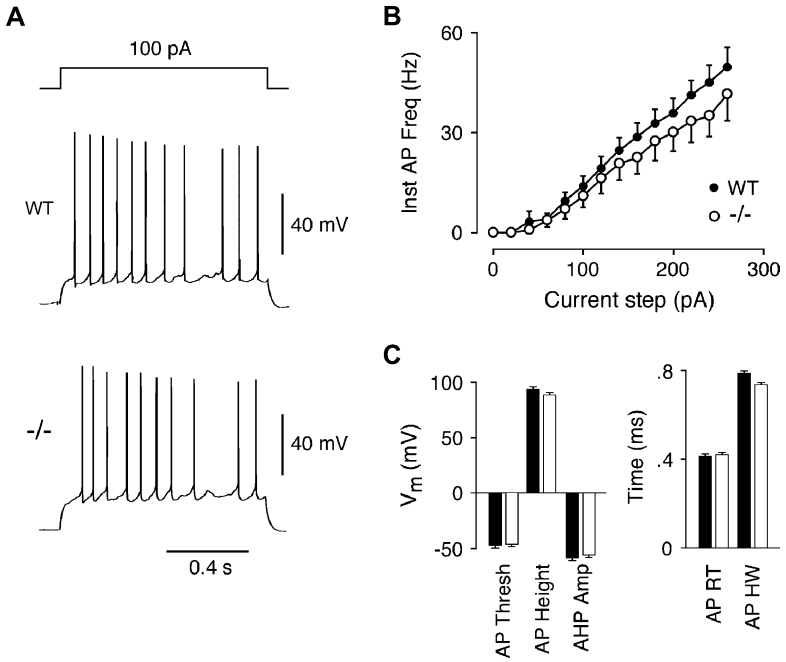

Fig. 3. Intrinsic excitability of CA1 hippocampal pyramidal neurons is unaltered in −/− mice compared to WT. (A) Illustrative action potentials (APs) elicited by a 1-s-long 100 pA current step applied to a CA1 pyramid in a WT (top) or −/− (bottom) mouse. (B) Averaged *f–I* plot obtained from data like in panel A, for WT ($n = 20$ cells, closed symbols) and −/− ($n = 12$, open symbols). The plots are not significantly different. (C) Summary of measurements made on trains of APs in WT ($n = 20$ cells, filled bars) and −/− ($n = 12$ cells, open bars). AP voltage threshold, height, risetime (RT) and halfwidth (HW), as well as afterhyperpolarization (AHP) amplitude, are all not significantly different in WT and −/−.

3. Results

3.1. EEG experiments

All knockout mice exhibited generalized tonic–clonic seizures, whereas no seizures were observed in control mice. These seizures were usually heralded by a 10–30-s period of behavioral arrest, followed by a variable amount of facial twitching, asymmetrical or unilateral jerking of the forelimbs, then generalized stiffening and jerking of all four limbs. The animals usually exhibited prolonged post-ictal hypoactivity. This seizure semiology was highly suggestive of a partial onset seizure not initially involving the motor cortex, followed by local spread, involvement of the ipsilateral motor cortex and then, finally, secondary generalization.

EEGs obtained during such events confirmed that the seizures had a focal onset, with seizure activity appearing as low amplitude fast activity in the middle or posterior EEG channel on one side of the head (Fig. 1B, arrows), followed by involvement of neighboring channels, then synchronization, slowing, and an increase in the amplitude of the epileptic discharges (Fig. 1A). The seizures terminated abruptly, with pronounced post-ictal flattening (Fig. 1A, right).

Most knockout mice were also observed to have episodes of sudden behavioral arrest, lasting for several seconds or up to several minutes. On behavioral grounds alone, this was often difficult to distinguish from normal periods of rest or inactivity, though subtle myoclonic jerks of the head were sometimes observed. EEG recordings showed that many episodes of behavioral freezing in the knockouts were associated with paroxysms of spike-and-slow wave (SSW) activity (Fig. 2A; cf. wildtype, Fig. 2B). Conversely, sustained runs of SSW were invariably associated with an interruption to normal exploratory behavior. During some hypokinetic events, individual SSW complexes were accompanied by a slight myoclonic head movement; this was often not apparent to visual inspection of the animal but was recorded on the piezoelectric movement trace (Fig. 2A, right). Interictal EEGs were also markedly affected by loss of functional GalR1. EEGs in knockout mice showed frequent stereotyped SSWs, whereas such events were rare in the wildtype control mice (Fig. 2D). Like the seizures, the SSWs had a focal distribution: the amplitude of individual events was usually greatest in one particular channel in the array and tapered off in neighboring channels, becoming undetectable at sites distant from the primary focus. In four of the seven knockout mice, one of the middle channels was implicated as the main source of spike-and-slow wave events; in the remaining three knockout mice a posterior channel was implicated. This is consistent with the hypothesis that the primary site of epileptogenesis in the knockout mice is in the temporal lobes but further studies with depth electrodes would be required to confirm the precise point of origin of the abnormalities. For individual knockout mice, the primary focus was not always constant, with SSW events occurring independently in both hemispheres. The frequency of the SSW complexes varied over a continuum, so that there was no clear distinction between interictal hypoactivity associated with frequent SSWs and actual hypokinetic seizures. Overall, there was a strong inverse correlation between movement in the knockout mice and the frequency of SSW events on EEG (Fig. 2C; $r = -0.77$,

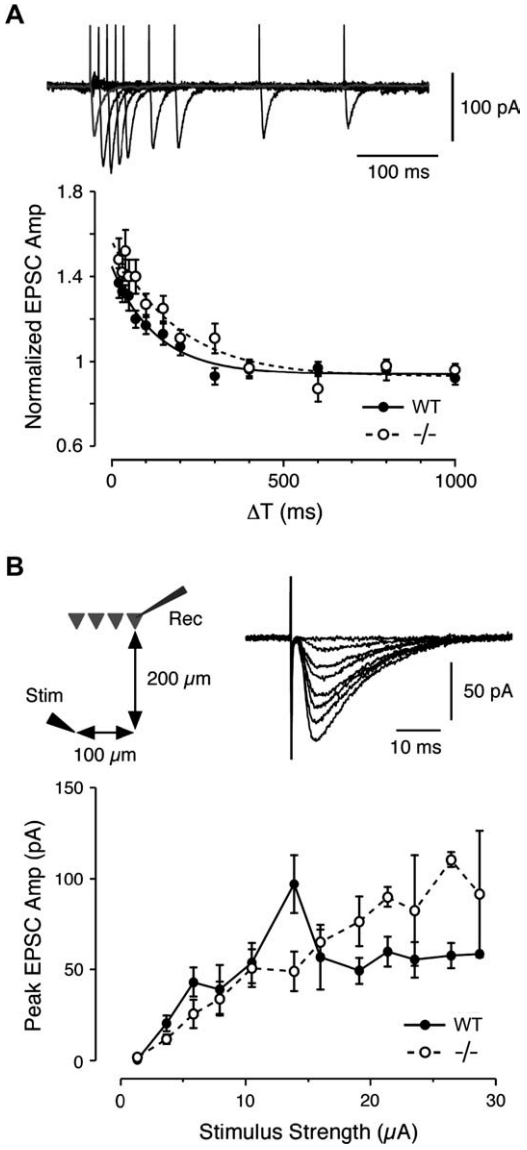

Fig. 4. Paired-pulse and stimulus–response properties of evoked EPSCs in CA1 pyramidal neurons are similar in WT and −/− mice. (A, top) Illustrative paired-pulse data from a WT neuron. Each trace is an average of five interleaved sweeps. The leftmost EPSC is the response to a single stimulus; remaining EPSCs are the responses to the second of the paired stimuli, after subtracting the response to the first. (A, bottom) Averaged paired-pulse data from WT ($n = 8$ cells, filled symbols) and −/− ($n = 7$ cells, open symbols). For each cell, EPSC amplitudes were normalized to the single-stimulus response recorded for that cell, then all normalized amplitudes at each ΔT were averaged together. Superimposed smooth curves are single-exponential fits with time constants 130 ms (WT) and 188 ms (−/−). There is little difference between the two plots. (B, top), Schematic (left) showing the placement of the stimulating electrode in *Str. radiatum* with respect to the postsynaptic neuron. The stimulating electrode was lowered ∼20 μm into the slice at this point. Illustrative EPSCs (right) evoked by a range of stimulus strengths (0–22 μA at 2–3 μA intervals) are shown at right; this was a WT cell. Each trace is an average of 20 sweeps. (B, bottom), Averaged stimulus–response plots from WT ($n = 7$ cells, filled symbols) and −/− ($n = 7$ cells, open symbols). There is no systematic difference between the two plots.

Pearson's correlation coefficient). Conversely, the infrequent SSW events observed in wildtype mice (Fig. 2D) were variable in morphology and distribution, with no clear focus, and there was no behavioral correlate. For periods in which no SSWs were observed, the interictal EEGs of knockout and wildtype mice were not distinguishable (data not shown).

Following automated counting of the SSW events and manual blinded rejection of misshapen events, a statistically significant difference in the mean frequency of SSW events was observed between the knockout and control mice, regardless of whether the activity was expressed as frequency of events detected in the most active channel of each mouse (9 ± 2 events/h, $n = 9$, for WT; 97 ± 33 events/h, $n = 7$, for −/−; Fig. 2D), or whether all events for each mouse were included, regardless of their location (26 ± 5 events/h, $n = 9$, for WT; 204 ± 67 events/h, $n = 7$, for −/−).

3.2. Slice experiments

Pyramidal neurons in the mid-CA1 region of ventral hippocampus were selected for study, based on their location in *Stratum pyramidale*, healthy appearance under IR-DIC optics, and characteristic spiking behavior. The resting membrane potential, measured shortly after adopting a whole-cell configuration, was not significantly different in WT and *Galr1*$^{-/-}$ neurons (-65.4 ± 0.5 mV, $n = 19$, for WT; -65.9 ± 1.0 mV, $n = 20$, for −/−). The input resistance was also not different between the two kinds of tissue (141 ± 9 MΩ for WT, 129 ± 14 MΩ for −/−). These results indicate that CA1 pyramidal neurons were equally healthy in both WT and knockout animals.

We first asked whether the epileptic phenotype of knockouts was related to altered intrinsic firing properties of CA1 pyramids. Intrinsic excitability was assessed by injecting a series of 1 s-long depolarizing current steps at the soma and making a plot of average instantaneous firing frequency versus amplitude of the current step (*f–I* plot; Fig. 3A, B). Averaged *f–I* plots for WT ($n = 20$) and −/− ($n = 12$) neurons were not significantly different (Fig. 3B). The AP voltage threshold, risetime, height and halfwidth were all unaltered between WT and −/− neurons, as was the absolute amplitude of the AHP between successive APs (Fig. 3C). Finally, the slow afterhyperpolarization (sAHP) measured following a 200-ms-long train of APs was not significantly different (1.5 ± 0.3 mV for WT, 2.3 ± 0.7 mV for −/−, $n = 6$).

We next addressed the possibility that altered neurotransmission in the CA1 region accompanied the epileptic phenotype. Paired pulses of presynaptic stimulation were applied to the Schaffer collaterals and the resultant postsynaptic currents were recorded in CA1 pyramidal neurons under voltage clamp (Fig. 4A). Differences in presynaptic determinants of transmitter release would be revealed by differences in paired-pulse facilitation or depression in the postsynaptic responses (Zucker, 1989). In a first series of experiments, no blockers were added to the bath solution and the internal solution contained 135 mM potassium methylsulfate. Under these conditions $GABA_A$ergic IPSCs were small because the cell was voltage clamped close to the chloride reversal potential (∼ −70 mV); hence, the response was primarily mediated by EPSCs. However, major alterations in $GABA_A$ergic

transmission, if present, would be revealed as changes in shunting inhibition (Kandel et al., 2000). There was little difference between WT and mutant cells (Fig. 4A): maximal paired-pulse facilitation of EPSCs was similar at $\Delta T = 20$ ms (1.37 ± 0.07, $n = 8$, for WT; 1.48 ± 0.10, $n = 7$, for $-/-$), and the time constants for recovery were also similar ($\tau = 130$ ms for WT, $\tau = 188$ ms for $-/-$; superimposed smooth curves, Fig. 4A). In a second series of experiments, the paired-pulse properties of IPSCs were measured directly by blocking EPSCs with CNQX (5 μM) and using internal solution containing 135 mM KCl. Again, there was no significant difference between WT and mutant cells ($n = 3$ of each; not illustrated). Together these experiments indicate that the short-term dynamics of neurotransmitter release are not different between WT and $-/-$ tissues.

In the above paired-pulse experiments the stimulus strength was adjusted to elicit similar-sized control EPSCs in both WT and mutant tissues (78.9 ± 5.4 pA for WT, 70.7 ± 6.5 pA for $-/-$). It remained possible that epileptic tissue shows an altered response to the *same* stimulus strength. This was tested by measuring stimulus–response data for EPSCs (Fig. 4B). Because such data may also depend on the placement of the extracellular stimulating electrode, we endeavored to be consistent, always placing the stimulator at a fixed location with respect to the postsynaptic neuron (inset, Fig. 4B). There was no consistent difference between the stimulus–response curves for WT and mutant neurons (Fig. 4B).

Finally, we compared the properties of spontaneous miniature EPSCs and IPSCs. These were often measured in normal external solution without addition of tetrodotoxin (TTX) to block spontaneous APs (Fig. 5). However, control experiments showed that addition of TTX (0.5 μM) had no effect on any of the measured properties of spontaneous EPSCs and IPSCs ($n = 3$), confirming that they were true miniature synaptic currents resulting from the random exocytosis of single vesicles of neurotransmitter (Sulzer and Pothos, 2000). Miniature EPSCs showed no change in either the average amplitude (17.8 ± 1.0 pA, $n = 8$, for WT; 19.4 ± 1.5 pA, $n = 6$, for $-/-$) or frequency (0.9 ± 0.2 Hz for WT; 1.0 ± 0.2 Hz for $-/-$) (Fig. 5A, right). On the other hand, miniature IPSCs had a significantly lower frequency in mutant tissue (3.8 ± 0.8 Hz, $n = 8$, for WT; 1.9 ± 0.4 Hz, $n = 11$, for $-/-$), whereas their average amplitude was not significantly different (42.1 ± 4.8 pA for WT; 42.2 ± 3.5 pA for $-/-$) (Fig. 5B). These results suggest that one aspect of synaptic inhibition is compromised in the hippocampus of *Galr1*$^{-/-}$ mice.

4. Discussion

In this paper we have characterized the electroencephalographic features of epileptic GalR1 knockout mice and studied the effect of the mutation on CA1 pyramidal cells of the ventral hippocampus.

The EEG analysis revealed that convulsive seizures in *Galr1*$^{-/-}$ mice have a partial onset with secondary generalization, that paroxysms of spike-and-slow waves occur and are correlated with hypoactivity, and that the interictal EEG is markedly abnormal, with frequent focal spike-and-slow

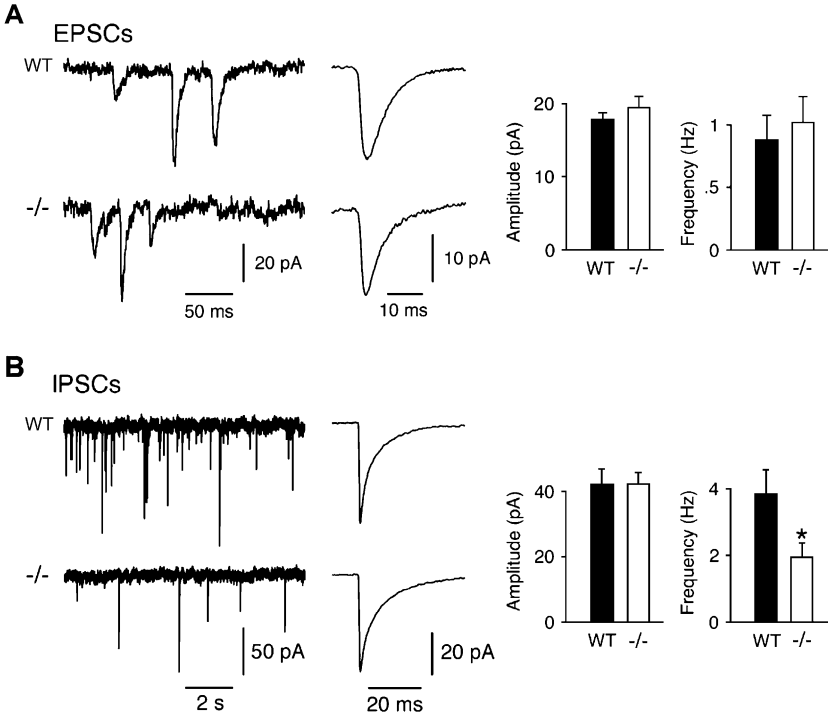

Fig. 5. Miniature EPSCs (mEPSCs) are identical in WT and $-/-$ CA1 pyramidal neurons, but miniature IPSCs (mIPSCs) are less frequent in $-/-$ neurons. (A) Segments of raw data (left) and averages of 89 and 151 captured mEPSCs (center), recorded in a WT (top) or $-/-$ (bottom) CA1 neuron. Bar graphs at right show the population average of the mean amplitude (left) or mean frequency (right) of mEPSCs recorded in $n = 8$ WT cells (filled bars) or $n = 6$ $-/-$ cells (open bars). (B) The same analysis was performed for mIPSCs. Averaged IPSCs (center) are averages of 80 and 134 captured mIPSCs. Bar graphs are population averages from $n = 8$ WT or $n = 11$ $-/-$ cells. The frequency of mIPSCs is significantly less in $-/-$ cells.

wave events. These findings are consistent with previous observations of the seizure phenotype (Jacoby et al., 2002b) and also with the hypothesis that the seizures originate focally, in structures such as the hippocampus that normally express GalR1. Further studies with depth electrodes are underway to pinpoint the seizure focus more precisely. Importantly, the epileptic phenotype in these animals correlates well with the clinical spectrum of partial (focal) epilepsies in humans and, in particular, with temporal lobe epilepsy. Subjects with temporal lobe epilepsy may have episodes of behavioral arrest and diminished awareness, or may progress to motor seizures with contralateral limb posturing or jerking, or to generalized tonic–clonic convulsions (Harlen, 1997).

The penetrance of epilepsy was 25% in the original colony of GalR1 knockout mice (Jacoby et al., 2002a,b) but further experience has shown that penetrance is not uniform: some *Galr1*$^{-/-}$ kindreds have close to 100% penetrance (this study), while others show no apparent spontaneous seizures while nonetheless having an altered seizure threshold (Mazarati et al., 2004a). Clearly, the GalR1 knockout mutation requires an appropriate genetic background to produce epilepsy. Discovering the relevant genes could reveal clues as to the mechanisms involved (Frankel, 1999; Kitami et al., 2004) and backcrossing experiments are underway to address this issue. The potential influence of genetic background should be kept in mind when considering mice with other mutations in the galanin system, such as galanin knockouts in which spontaneous seizures were not observed but seizure threshold was reduced (Mazarati et al., 2000).

GalR2 receptors have also been implicated in the anticonvulsant effects of galanin (Mazarati, 2004). Local down-regulation of GalR2 in the hippocampus, using antisense oligonucleotides, lowers the threshold for induced seizures in mice (Mazarati et al., 2004b), while nominally GalR2-preferring agonists have the opposite effect (Mazarati et al., 1998, 2004b). Although GalR1 and GalR2 both mediate anticonvulsant activity, differences in their distribution (Burgevin et al., 1995; Parker et al., 1995; O'Donnell et al., 1999) and physiology (Branchek et al., 2000) suggest that they achieve this by different mechanisms.

It is striking that seizures in GalR1 mice have a delayed and variable onset, typically appearing after 3 weeks and with a mean age of onset of 11 weeks (Jacoby et al., 2002a). Changes in GalR1 expression may be involved but, in postnatal rats, the expression of GalR1 mRNA has been reported to change little during development (Burazin et al., 2000). As with the variable penetrance of the epileptic phenotype, it is likely that the factors determining the age of onset are complex, involving genetic, environmental and stochastic elements.

In our slice studies, we sought to identify electrophysiological changes associated with epilepsy in GalR1 knockout mice. We focused on CA1 pyramidal neurons in the ventral hippocampus because these normally express a high density of GalR1 in rodents (Burgevin et al., 1995; Parker et al., 1995; Hohmann et al., 2003) and because the hippocampus has been implicated in other forms of seizure activity (Dudek et al., 1999). Both of these factors should act in favor of our finding alterations in CA1 pyramids following the knockout of the *Galr1* gene. Perhaps surprisingly, we found only a mild electrophysiological change in these neurons. Resting potential, input resistance, short-term synaptic plasticity, excitatory synaptic input–output curves, miniature EPSC frequency and amplitude, sAHP amplitude, and several properties of APs were all unchanged. The notable difference between the two genotypes was in the frequency of miniature IPSCs recorded in pyramidal cells, which was significantly reduced in the knockout mice. This suggests that inhibitory activity in the knockout mice may be reduced, a change that would be expected to enhance the risk of seizures.

Changes following the disruption of GalR1 are likely to fall into two categories: (i) changes directly due to the mutation, and (ii) changes secondary to seizures. Considering the direct changes, there have been several reports on the acute effect of galanin on hippocampal slices, most of them using bath-applied galanin or weakly specific antagonists. Dutar et al. (1989) showed that galanin (1–5 μM) had little effect on the passive electrical properties of ventral CA1 pyramids and weakly depressed fast excitatory and inhibitory synaptic transmission, but blocked by about 60% the slow cholinergic EPSP. Because this EPSP is typically evoked by strong stimulation (0.5 s at 20–30 Hz) in the presence of eserine, it would not have been visible under our conditions.

Zini et al. (1993) reported that potassium-evoked release of glutamate from hippocampal slices (assayed chemically) is inhibited 50–60% by galanin (0.3 μM), suggesting that the peptide has a presynaptic inhibitory effect at some glutamatergic terminals (see also Mazarati et al., 2000). Electrophysiological evidence for this effect was provided by Kokaia et al. (2001) who reported that frequency facilitation of EPSPs at mossy fiber-CA3 synapses was reduced in galanin-overexpressing transgenic mice, an effect that was blocked by the galanin receptor antagonist M35. However, M35 did not enhance frequency facilitation in WT animals, suggesting that there is little tonic inhibition of glutamate release from mossy fibers when galanin levels are normal (Kokaia et al., 2001). Coumis and Davies (2002) also reported that galanin had no effect on basal excitatory or inhibitory synaptic transmission. This is in accord with our finding that synaptic strength and short-term plasticity were unaffected in the *Galr1*$^{-/-}$ mice.

Other experiments have explored galanin's influence on long-term potentiation (LTP) and depression (LTD) in hippocampal slices. Low concentrations of galanin (100–200 nM) were found to inhibit the induction of LTP in area CA1, with no effect on LTD (Sakurai et al., 1996; Coumis and Davies, 2002). Recently, a non-peptide galanin agonist with a preference for GalR1, galmic, was reported to inhibit the induction of LTP in the hippocampus (Bartfai et al., 2004). In contrast, galanin antagonists have no effect on CA1 LTP, suggesting that plasticity in this region is unaffected by tonic low levels of galanin (cf. dentate gyrus; Mazarati et al., 2000). It might be expected, however, that galanin levels would be locally increased during intense neural firing, given the propensity of neuropeptides to be released under such conditions (see Baraban and Tallent, 2004, for a review). If so, by inhibiting

synaptic potentiation under conditions of high frequency firing, galanin could limit the risk of a positive feedback loop in which spontaneous episodes of high frequency firing cause excessive synaptic potentiation, leading to further neural activity and epileptogenesis. Thus, on the basis of previous reports, endogenous galanin could inhibit seizures acutely, by reducing glutamate and acetylcholine release from hippocampal inputs, and it could also provide a safeguard against chronic epileptogenesis by inhibiting synaptic potentiation.

Turning now to chronic changes following seizures in GalR1 knockout mice, what electrophysiological alterations might be expected? Some clues can be obtained from recent studies in a related colony of GalR1 knockout mice. Mazarati et al. (2004a) reported that their *Galr1*$^{-/-}$ mice, originally descended from the same colony as those described here, do not exhibit spontaneous seizures but instead show enhanced seizures in response to a variety of stimuli including Li-pilocarpine and perforant pathway stimulation, but not kainic acid. As these authors point out, the lack of heightened susceptibility to kainic acid-induced seizures is understandable given that this glutamate agonist acts directly on postsynaptic receptors to cause depolarisation and cellular firing, whereas galanin is implicated as a presynaptic inhibitor of glutamate release; kainic acid thus bypasses the step at which galanin might modify excitability. Conversely, the susceptibility of the knockout mice to status epilepticus following perforant pathway stimulation and their susceptibility to cholinergic stimulation with pilocarpine are consistent with the postulated roles of galanin in inhibiting glutamate release and in suppressing postsynaptic responses to acetylcholine.

Of particular interest to us was the authors' observation that knockout mice had a heightened susceptibility to seizure-induced injury to CA1 pyramidal cells, dentate granule cells and hilar interneurons (Mazarati et al., 2004a). This did not appear to be due solely to the occurrence of more severe seizures in the knockouts, and might reflect a neuroprotective role of galanin. Such a role has also been suggested by Elliott-Hunt et al. (2004). In a different study by Mazarati et al. (2004b), GalR2 knockdown enhanced loss of hilar interneurons, suggesting that both major galanin receptor subtypes may affect susceptibility to cellular injury. These findings correlate well with our own observation that hippocampal pyramidal cells in GalR1 knockouts with chronic epilepsy have a reduced frequency of GABAergic miniature IPSCs (mIPSCs). The loss of interneurons in the hippocampus would be expected to reduce the number of inhibitory synapses contacting each pyramidal cell (unless surviving interneurons compensated by sprouting new axonal branches) and this could lead to a reduced frequency of mIPSCs. Other possible explanations of a reduced frequency of mIPSCs could be that the lack of GalR1 during embryogenesis has altered the number of inhibitory synapses on each pyramidal cell, or that inhibitory synapses have been lost independent of seizure-induced injury. These hypotheses will be assessed in future studies involving detailed morphological assessment of inhibitory synapses in the hippocampus of GalR1 knockout mice and a comparison of seizure-prone GalR1 knockouts with nonepileptic GalR1 knockouts.

In summary, this study has shown that GalR1 knockout mice of the appropriate genetic background exhibit spontaneous partial seizures, with a varying extent of secondary generalization, and thus make an attractive model for studying partial epilepsy. In addition to previously proposed mechanisms for the anticonvulsant actions of galanin, we have shown that such mice have reduced inhibition in the hippocampus. It is likely that further clues to the mechanism of seizure generation in the *Galr1*$^{-/-}$ mouse will come from studies of a variety of brain regions, in which our examination of CA1 pyramidal neurons is a first step. In the meantime, the continued interest of pharmaceutical companies in developing galanin agonists as potential therapeutic agents seems well justified.

Acknowledgements

This work was supported by recurrent funding from the John Curtin School of Medical Research (JMB) and from the National Health and Medical Research Council of Australia (ASJ, JS, TPI). CDM is the recipient of an ANU PhD Scholarship.

References

Baraban, S.C., Tallent, M.K., 2004. Interneuronal neuropeptides – endogenous regulators of neuronal excitability. Trends Neurosci. 27, 135–142.

Bartfai, T., Lu, X., Badie-Mahdavi, H., Barr, A.M., Mazarati, A., Hua, X.Y., et al., 2004. Galmic, a nonpeptide galanin receptor agonist, affects behaviors in seizure, pain, and forced-swim tests. Proc. Natl Acad. Sci. U.S.A. 101, 10470–10475.

Bekkers, J.M., Delaney, A.J., 2001. Modulation of excitability by α-dendrotoxin-sensitive potassium channels in neocortical pyramidal neurons. J. Neurosci. 21, 6553–6560.

Branchek, T.A., Smith, K.E., Gerald, C., Walker, M.W., 2000. Galanin receptor subtypes. Trends Pharmacol. Sci. 21, 109–117.

Burazin, T.C., Larm, J.A., Ryan, M.C., Gundlach, A.L., 2000. Galanin-R1 and -R2 receptor mRNA expression during the development of rat brain suggests differential subtype involvement in synaptic transmission and plasticity. Eur. J. Neurosci. 12, 2901–2917.

Burgevin, M.-C., Loquet, I., Quarteronet, D., Habert-Ortoli, E., 1995. Cloning, pharmacological characterization, and anatomical distribution of a rat cDNA encoding for a galanin receptor. J. Mol. Neurosci. 6, 33–41.

Clements, J.D., Bekkers, J.M., 1997. Detection of spontaneous synaptic events using an optimally scaled template. Biophys. J. 73, 220–229.

Coumis, U., Davies, C.H., 2002. The effects of galanin on long-term synaptic plasticity in the CA1 area of rodent hippocampus. Neuroscience 112, 173–182.

Crawley, J.N., 1996. Galanin–acetylcholine interactions: relevance to memory and Alzheimer's disease. Life Sci. 58, 2185–2199.

Dudek, F.E., Patrylo, P.R., Wuarin, J.-P., 1999. Mechanisms of neuronal synchronization during epileptiform activity. Adv. Neurol. 79, 699–708.

Dutar, P., Lamour, Y., Nicoll, R.A., 1989. Galanin blocks the slow cholinergic EPSP in CA1 pyramidal neurons from ventral hippocampus. Eur. J. Pharmacol. 164, 355–360.

Elliott-Hunt, C.R., Marsh, B., Bacon, A., Pope, R., Vanderplank, P., Wynick, D., 2004. Galanin acts as a neuroprotective factor to the hippocampus. Proc. Natl Acad. Sci. U.S.A. 101, 5105–5110.

Frankel, W.N., 1999. Detecting genes in new and old mouse models for epilepsy: a prospectus through the magnifying glass. Epilepsy Res. 36, 97–110.

Haberman, R.P., Samulski, R.J., McCown, T.J., 2003. Attenuation of seizures and neuronal death by adeno-associated virus vector galanin expression and secretion. Nat. Med. 9, 1076–1080.

Harlen, J., 1997. Diagnosis and Management of Epilepsy in Adults. Scottish Intercollegiate Guidelines Network, Edinburgh, pp. 1–59.

Hohmann, J.G., Jureus, A., Teklemichael, D.N., Matsumoto, A.M., Clifton, D.K., Steiner, R.A., 2003. Distribution and regulation of galanin receptor 1 messenger RNA in the forebrain of wild type and galanin-transgenic mice. Neuroscience 117, 105–117.

Iismaa, T.P., Shine, J., 1998. Galanin and galanin receptors. Regulatory Peptides and Cognate Receptors. Springer, pp. 257–291.

Jacoby, A.S., Holmes, F.E., Hort, Y.J., Shine, J., Iismaa, T.P., 2002a. Phenotypic analysis of *Galr1* knockout mice reveals a role for GALR1 galanin receptor in modulating seizure activity but not nerve regeneration. Lett. Pept. Sci. 8, 139–146.

Jacoby, A.S., Hort, Y.J., Constantinescu, G., Shine, J., Iismaa, T.P., 2002b. Critical role for GALR1 galanin receptor in galanin regulation of neuroendocrine function and seizure activity. Mol. Brain Res. 107, 195–200.

Jungnickel, S.R., Gundlach, A.L., 2005. [^{125}I]-Galanin binding in brain of wildtype, and galanin- and GalR1-knockout mice: strain and species differences in GalR1 density and distribution. Neuroscience 131, 407–421.

Kandel, E.R., Schwartz, J.H., Jessell, T.M., 2000. Principles of Neural Science. McGraw-Hill/Appleton & Lange, 1414 pp.

Kitami, T., Ernest, S., Gallaugher, L., Friedman, L., Frankel, W.N., Nadeau, J.H., 2004. Genetic and phenotypic analysis of seizure susceptibility in PL/J mice. Mamm. Genome 15, 698–703.

Kokaia, M., Holmberg, K., Nanobashvili, A., Xu, Z.-Q.D., Kokaia, Z., Lendahl, U., et al., 2001. Suppressed kindling epileptogenesis in mice with ectopic overexpression of galanin. Proc. Natl Acad. Sci. U.S.A. 98, 14006–14011.

Macdonald, R.L., 1999. Cellular actions of antiepileptic drugs. Antiepileptic Drugs, Pharmacology and Therapeutics. Springer-Verlag, pp. 123–150.

Mazarati, A., Lu, X., Shinmei, S., Badie-Mahdavi, H., Bartfai, T., 2004a. Patterns of seizures, hippocampal injury and neurogenesis in three models of status epilepticus in galanin receptor type 1 (GalR1) knockout mice. Neuroscience 128, 431–441.

Mazarati, A., Lu, X., Kilk, K., Langel, U., Wasterlain, C., Bartfai, T., 2004b. Galanin type 2 receptors regulate neuronal survival, susceptibility to seizures and seizure-induced neurogenesis in the dentate gyrus. Eur. J. Neurosci. 19, 3235–3244.

Mazarati, A.M., 2004. Galanin and galanin receptors in epilepsy. Neuropeptides 38, 331–343.

Mazarati, A.M., Wasterlain, C.G., 2002. Anticonvulsant effects of four neuropeptides in the rat hippocampus during self-sustaining status epilepticus. Neurosci. Lett. 331, 123–127.

Mazarati, A.M., Halászi, E., Telegdy, G., 1992. Anticonvulsive effects of galanin administered into the central nervous system upon the picrotoxin-kindled seizure syndrome in rats. Brain Res. 589, 164–166.

Mazarati, A.M., Liu, H., Soomets, U., Sankar, R., Shin, D., Katsumori, H., et al., 1998. Galanin modulation of seizures and seizure modulation of hippocampal galanin in animal models of status epilepticus. J. Neurosci. 18, 10070–10077.

Mazarati, A.M., Hohmann, J.G., Bacon, A., Liu, H., Sankar, R., Steiner, R.A., et al., 2000. Modulation of hippocampal excitability and seizures by galanin. J. Neurosci. 20, 6276–6281.

Mennicken, F., Hoffert, C., Pelletier, M., Ahmad, S., O'Donnell, D., 2002. Restricted distribution of galanin receptor 3 (GalR3) mRNA in the adult rat central nervous system. J. Chem. Neuroanat. 24, 257–268.

O'Donnell, D., Ahmad, S., Wahlestedt, C., Walker, P., 1999. Expression of the novel galanin receptor subtype GALR2 in the adult rat CNS: distinct distribution from GALR1. J. Comp. Neurol. 409, 469–481.

Parker, E.M., Izzarelli, D.G., Nowak, H.P., Mahle, C.D., Iben, L.G., Wang, J., et al., 1995. Cloning and characterization of the rat GALR1 galanin receptor from Rin14B insulinoma cells. Mol. Brain Res. 34, 179–189.

Sakurai, E., Maeda, T., Kaneko, S., Akaike, A., Satoh, M., 1996. Galanin inhibits long-term potentiation at Schaffer collateral-CA1 synapses in guinea-pig hippocampal slices. Neurosci. Lett. 212, 21–24.

Sander, J.W., 2004. The use of antiepileptic drugs – principles and practice. Epilepsia 45 (Suppl. 6), 28–34.

Schött, P.A., Hökfelt, T., Ögren, S.O., 2000. Galanin and spatial learning in the rat. Evidence for a differential role for galanin in subregions of the hippocampal formation. Neuropharmacology 39, 1386–1403.

Sulzer, D., Pothos, E.N., 2000. Regulation of quantal size by presynaptic mechanisms. Rev. Neurosci. 11, 159–212.

Wasterlain, C.G., Mazarati, A.M., Naylor, D., Niquet, J., Liu, H., Suchomelova, L., et al., 2002. Short-term plasticity of hippocampal neuropeptides and neuronal circutiry in experimental status epilepticus. Epilepsia 43 (Suppl. 5), 20–29.

Wynick, D., Thompson, S.W.N., McMahon, S.B., 2001. The role of galanin as a multi-functional neuropeptide in the nervous system. Curr. Opin. Pharmacol. 1, 73–77.

Zini, S., Roisin, M.P., Langel, U., Bartfai, T., Ben-Ari, Y., 1993. Galanin reduces release of endogenous excitatory amino acids in the rat hippocampus. Eur. J. Pharmacol. 245, 1–7.

Zucker, R.S., 1989. Short-term synaptic plasticity. Annu. Rev. Neurosci. 12, 13–31.